DOI: 10.1002/ejic.200900023

Oxido Pincer Ligands – Exploring the Coordination Chemistry of Bis(hydroxymethyl)pyridine Ligands for the Late Transition Metals

Axel Klein,*[a] Said Elmas,[a] and Katharina Butsch[a]

Keywords: N,O ligands / Ligand design / Transition metals / Binding modes / UV/Vis spectroscopy

Coordination of the 2,6-bis(hydroxymethyl)pyridine-based oxido pincer ligands RR′pydimH_2 [R = R′ = H (pydimH_2); R = R′ = Me (pydipH_2); R = 2-tolyl, R′ = Me (pydotH_2)] towards late transition metals Co^{II}, Ni^{II}, Cu^{II}, Zn^{II}, Pd^{II} and Pt^{II} allows the formation of molecular species (complexes), which exhibit three main structural motifs in the solid state. The two main species are pentacoordinate [(RR′pydimH_2)MCl_2] and hexacoordinate [(RR′pydimH_2)$_2$M]X_2, both of which are stable in solution and can be interconverted by changing the solvent polarity. The disproportionation equilibrium [(RR′pydimH_2)MCl_2] ⇌ [(RR′pydimH_2)$_2$M]$^{2+}$ + $[MCl_4]^{2-}$ was studied by optical spectroscopy. The chiral ligand pydotH_2 allows the formation of chiral complexes. In the square-planar complexes [(pydimH_2)$_2MCl_2$] (M = Pd^{II} or Pt^{II}) the oxido donor functions of the ligands do not take part in the coordination.

Introduction

Tridentate ligands of the so-called pincer type combine the possibility of preparing highly stable transition metal complexes with defined stereochemistry with almost unlimited possibilities for ligand derivatisation and fine-tuning of the properties of these complexes. This has allowed the rational design of such complexes for applications in catalysis or molecular sensing.[1,2] Initially coined for E^C^E donor combinations with E = N, S, P or O and comprising a central M–C bond,[1] the term "pincer ligand" has since been extended to any combination of donor atoms from the periodic table.[2] The vast majority of pincer complexes are, however, restricted to combinations of C, N, P or S donors, and the use of O-donor functions is far less developed. The main reason for this choice is the expected (and found) high stability of complexes of the so called "soft" donors C, N, P and S in combination with the rather "soft" late transition metals (groups 8–11, 4d or 5d elements), in agreement with the completely empirical but highly intuitive HSAB concept.[3] This concept suggests that the binding of these metals to O donor atoms is likely to be weak, therefore it is not surprising to find a relatively small number of complexes of late transition metals with oxido pincer ligands.

Oxido pincer ligands based on 2,6-bis(hydroxymethyl)-pyridine (pydimH_2, Scheme 1), which has an O^N^O donor set, provide a number of interesting features for coordination chemistry and the application of their complexes. Firstly, the possibility of substituting the protons on the methylene C atom allows interesting electronic and steric variations to be introduced into ligands RR′pydimH_2 (Scheme 1) and their complexes. The most interesting variation is surely the introduction of one alkyl, aryl or alkynyl group, which leads to two stereogenic centres (R = H, R′ = alkyl, aryl, alkynyl). Alternatively, chiral disubstituted pydimH_2 derivatives have been created by using menthyl or other chiral groups. These have been used in several studies with early transition metal ions such as Ti^{IV},[4] Zr^{IV},[5,6] Hf^{IV},[6] V^{V}[7] or Mo^{VI}.[7,8] Another interesting aspect of ligands of the RR′pydimH_2 type is the possibility of stepwise deprotonation upon coordination, which goes along with increasing hardness of the metal ion. Examples for complexes of early transition metals containing exclusively the fully deprotonated ligand dianion RR′pydim^{2-} include [Ti(RR′pydim)$_2$], [Ti(RR′pydim)X_2] (R = R′ = Ph, H; X = Cl or O*i*Pr),[9] [Cp*Ti(L)(pydim)], [Cp*Ti(L′)(pydim)]$^+$ (Cp* = pentamethylcyclopentadienide; L = Me, OH; L′ = H_2O, MeCN),[10] Na[VO_2(pydim)],[11] [Cp*Ta(Me)(pydim)(X)] (X = OTf, H_2O),[10] [MoO_2(pydim)][12] or the above-mentioned chiral complexes.

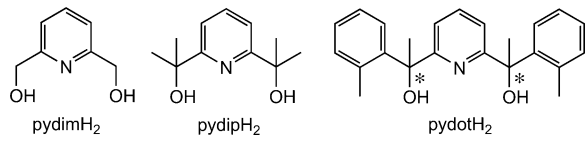

Scheme 1. O,N,O oxido pincer ligands used in this study. 2,6-Bis(hydroxymethyl)pyridine (pydimH_2), 2,6-bis(1-hydroxy-1-methylethyl)pyridine (pydipH_2) and 2,6-bis(1-hydroxy-1-*o*-tolylethyl)pyridine (pydotH_2).

[a] Universität zu Köln, Institut für Anorganische Chemie, Greinstrasse 6, 50939 Köln, Germany
E-mail: axel.klein@uni-koeln.de

Supporting information for this article is available on the WWW under http://www.eurjic.org or from the author.

In contrast to this, late transition metals usually coordinate to RR′pydimH_2 in its protonated form, as in [M(pydimH_2)$_2$]$^{2+}$ (M = Co, Ni, Cu, Zn)[13–15] [Cu($O_2CCH_2CH_3$)$_2$(pydimH_2)],[16] [Cu(nif)$_2$(pydimH_2)] {nif = niflumate, 2-{[3-(trifluoromethyl)phenyl]amino}nicotinate},[17] or [Cu(pydic)(pydimH_2)].[18] Exceptions to this rule have been found for the Cu^{II} complexes [Cu$_2$(η^2,μ-pydimH)$_2$(η^3-pydimH_2)$_2$]$^{2+}$[14b,19] and [Cu(pydimH_2)(pydimH)]$^+$.[14b]

An intermediate case arises in the polynuclear manganese complexes (and molecular magnets) [Mn$_9$($O_2CCH_2CH_3$)$_{12}$(pydim)(pydimH)$_2$(L)$_2$] {LH_2 = [6-(hydroxymethyl)-pyridin-2-yl](6-hydroxypyridin-2-ylmethoxy)methanol}[20] or [Mn$_4$(O_2CCH_3)$_2$(pydimH)$_6$](ClO_4)$_2$,[21] where the monodeprotonated ligand pydimH$^-$ is found. This agrees nicely with our general rule of deprotonation and increasing hardness. Again, however, there is an exception: the fully protonated ligand pydimH_2 is found in [MnCl(η^3-pydimH_2)(η^2-pydimH_2)]$^+$,[22] even though the complex also contains Mn^{II}, as in the examples with the partly deprotonated ligand.

At the far end of metal softness, the metal ions Pd^{II} and Pt^{II} have been found to coordinate only through the pyridine N-atom in complexes [MCl$_2$(pydimH_2)$_2$] (M = Pd[23] or Pt[24]); coordination of the hard O-donor functions was not observed.

In this paper we report on a study focussing on the coordination chemistry of three simple oxido pincer ligands based on 2,6-bis(hydroxymethyl)pyridine (Scheme 1) towards late transition metals Co^{II}, Ni^{II}, Cu^{II}, Zn^{II}, Pd^{II} and Pt^{II}, which have an increasing "soft" character along the series. Within this series of ligands, the steric bulk at the methyloxy C atom and the basicity of this atom increases from pydimH_2 to pydipH_2 and pydotH_2 (Scheme 1), and pairs of enantiomers are expected for complexes of the pydotH_2 ligand.

The ligand pydipH_2 has been synthesised previously by lithiation of 2,6-dibromopyridine and addition of acetone in situ.[25] The method was first mentioned by Osborn and Kress (using menthone instead of acetone)[5,7] and has been developed recently by Schmalz et al. to a broadly applicable method, coined the "in situ quench (ISQ)" method.[25] The ligand pydipH_2 was alternatively recently prepared from dimethyl pyridine-2,6-dicarboxylate and MeLi.[26]

Results and Discussion

Synthesis of the Ligands

Whereas the ligand pydimH_2 is commercially available, pydipH_2 was synthesised from dimethyl pyridine-2,6-dicarboxylate and MeLi by modifying a literature procedure (Scheme 2).[26] The ligand pydotH_2 was prepared by using the ISQ method starting from 2,6-diacetylpyridine and tolylmagnesium bromide.

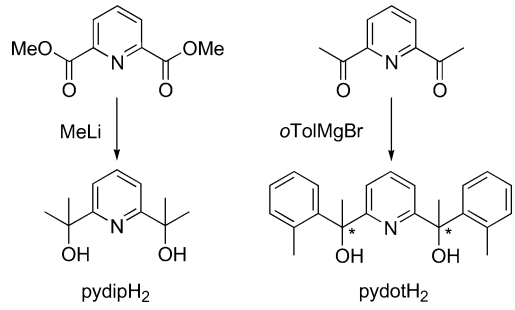

Scheme 2. Synthesis of the ligands pydipH_2 and pydotH_2.

Both ligands were obtained in good to excellent yields and fully characterised by elemental analysis and ^{1}H and ^{13}C NMR spectroscopy (see Experimental Section).

Crystal and Molecular Structure of pydotH_2

Suitable crystals of the ligand pydotH_2 were obtained from a concentrated solution in ethanol. The crystal structure was solved in the triclinic space group $P\bar{1}$. Close H···O contacts between hydroxy groups of two neighbouring molecules are observed in the crystal structure, although the H···O distances of 2.075(7) and 2.260(6) Å [O···O distance: 2.879(4) Å] qualify them as medium to weak H bonds.[27] The H atoms on O1 and O2 were found during refinement, whereas other H atoms were added by using appropriate riding models, Figure 1 shows the molecular structure.

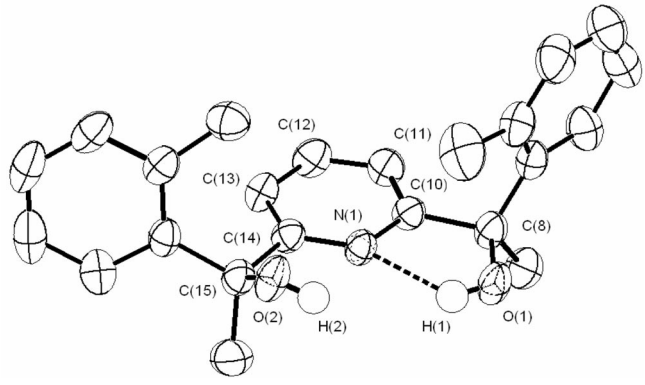

Figure 1. View of the molecular structure of pydotH_2 (thermal ellipsoids represent 30% probability). The H atoms on O1 and O2 are displayed, whereas others have been omitted for clarity. The dotted line represents the H bond of 2.016(3) Å [angle O(1)–H(1)···N(1) 123.0(2)°; N···O 2.557(5) Å].

One of the two hydroxy units (O1) in the free ligand pydotH_2 is almost co-planar with the pyridine core [tilt angle OCCN 2.57(2)°]. This is probably caused by a short O–H···N contact of 2.016(3) Å [angle N···H–O 123.0(2)°] which can be qualified as a medium to strong H bond.[27] The other hydroxy group is tilted away from the pyridine plane with a tilt angle of 37.59(2)°. Consequently, the O–H···N hydrogen bond is longer [2.426(3) Å; angle 103.0(2)°; N···O 2.729(5) Å] and thus much weaker. The methyl substituents of the two tolyl groups are both oriented towards

the core of the pincer ligand and, most importantly, in the crystal structure we find only the *meso* configuration of the molecule, with C8 in the (*R*) configuration and C15 in the (*S*) configuration.

Synthesis of the Metal Complexes

Ethanol turned out to be the best solvent to dissolve both the organic ligand and the metal chlorides. Complexes of the type [(RR′pydimH_2)MCl_2] (Scheme 3, Route A; M = Co, Ni, Cu, Zn) were synthesised by mixing solutions of the ligands with 3d metal salts in a 1:1 ratio (see Experimental Section for details). Alternatively, complexes of the composition [(RR′pydimH_2)$_2$M][MCl_4] were obtained by the same procedure for some of the ligands with M = Co and Zn (Route B1). Similarly, the application of a ligand/metal ratio of 2:1 allowed the formation of complexes [(RR′pydimH_2)$_2$M]Cl_2 (Route B2).

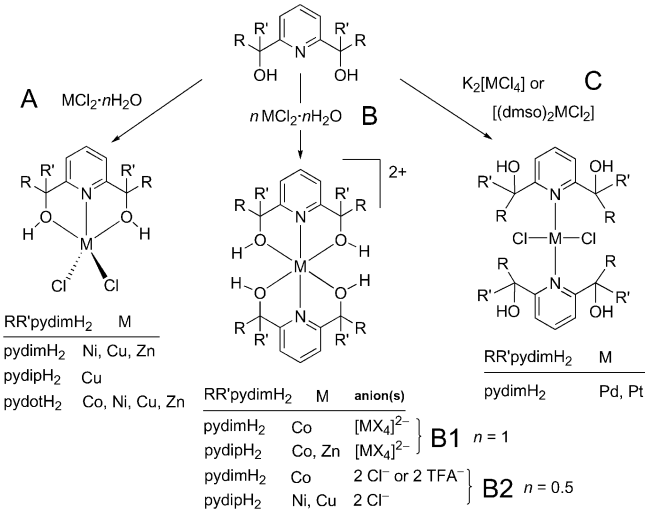

Scheme 3. Formation of the metal complexes.

The reaction of $K_2[MCl_4]$ (M = Pd or Pt) with pydimH_2 gave complexes of the composition [(pydimH_2)$_2$$MCl_2$] (Route C); the Pt complex has been described before.[24] The other ligands did not react under the chosen conditions (stirring at ambient temperature), therefore the alternative complex precursors [(dmso)$_2$$MCl_2$] were used, but again the reactions with pydipH_2 or pydotH_2 failed. The products obtained from the reaction of these precursors with pydimH_2 were the novel complexes *trans*-[(pydimH_2)$_2$$PdCl_2$] and *cis*- and *trans*-[(pydimH_2)(dmso)$PtCl_2$] (obtained as a mixture). The oxidation state of the metal atom remained unchanged, and the RR′pydimH_2 ligand remained protonated in all these reactions.

Crystal and Molecular Structures of the Complexes in the Solid State

The crystal structures discussed in this section were solved in various space groups ranging from triclinic $P\bar{1}$ to monoclinic *C*2/*c* (see Tables 3, 4 and 5 in the Experimental Section for details). Importantly, during the refinement process we were able to find all H atoms of the ligands' OH functions. Other H atoms were usually refined by using appropriate riding models. For the discussion of the crystal and molecular structures we will divide the structures into the three groups A, B and C defined in Scheme 3.

The first type (A) contains the structures of the neutral complexes [(RR′pydimH_2)MCl_2] (Figure 2). Most of them crystallised as solvates (EtOH or H_2O), and two polymorphs ($P2_1/c$ or $P\bar{1}$) of the compound [(pydimH_2)$ZnCl_2$] were crystallised and characterised (see Table 3 for details). The latter suggests that the space groups are probably not of particular importance for the structure discussion. There are frequent but weak H bonding interactions between the solvent molecules and the complexes or between complex molecules. The shortest contacts are observed between O–H protons and chlorido ligands in [(pydotH_2)$CoCl_2$]·EtOH, with an H···Cl distance of 2.054(8) Å [O···Cl 3.094(5) Å] and a Cl···H–O angle of 170.9(4)°, which classifies this interaction as a medium to strong H bond.[27] All the complexes exhibit a fivefold coordination sphere around the central metal atom with quite similar M–N and M–O distances between 1.93 and 2.07 Å for the M–N bonds and 2.00 and 2.22 Å for the M–O bonds (see Table 1). The pyridine ring and the oxido donor function of the RR′pydim ligands are almost coplanar and the NOMN coordination plane is perpendicular to the ClMCl plane.

A marked difference can be observed in the orientation of the chlorido co-ligands. Thus, the two chlorido ligands complete a trigonal-bipyramidal arrangement around the central metal atom for Co, Ni and Zn, whereas Cu displays a square-pyramidal coordination sphere (see Figure 2). Both polyhedra are distorted, with the Cl–M–Cl angle for the trigonal bipyramids varying from 113° to 118°. For the N–M–Cl angle, a smaller (102–117°) and a larger angle (128–145°) add up to a sum of about 245°. The square-pyramidal structure of the Cu^{II} derivative is characterised by a small Cl–M–Cl angle of 101.24(3)° and a large N–M–Cl angle of 165.16(5)°. The difference between Co, Ni and Zn on the one hand and the Cu^{II} derivative on the other can easily be explained by the d^9 configuration of Cu^{II}, with the expected Jahn–Teller distortion leading to a preferred 4 (square planar) + 1 coordination. Indeed, the axial chlorido ligand exhibits a markedly elongated distance [2.696(8) Å] compared to its equatorial counterpart [2.208(8) Å]. Interestingly, the O–M–O angle seems to be rather flexible, ranging from 144° to 160°. As expected, the highest value is found for the square-pyramidal Cu^{II} system. Furthermore, the chiral pydotH_2 ligand in the molecular structure of [(pydotH_2)$CoCl_2$]·EtOH (Figure 2) displays a *meso* configuration.

The second type of structure (B) is found for those of the composition [(RR′pydimH_2)$_2$M][X]$_n$, where X can be various anions like Cl, as in [(pydipH_2)$_2$Cu]Cl_2·H_2O (see Figure 3), or trifluoroacetic acid (TFA), as in [(pydimH_2)$_2$Co][TFA]$_2$. Alternatively, tetrachloridometallates $[MCl_4]^{2-}$ can act as counterion, as in [(pydipH_2)$_2$Co][$CoCl_4$] (see Table 4 for details of the crystal structures). Various hydro-

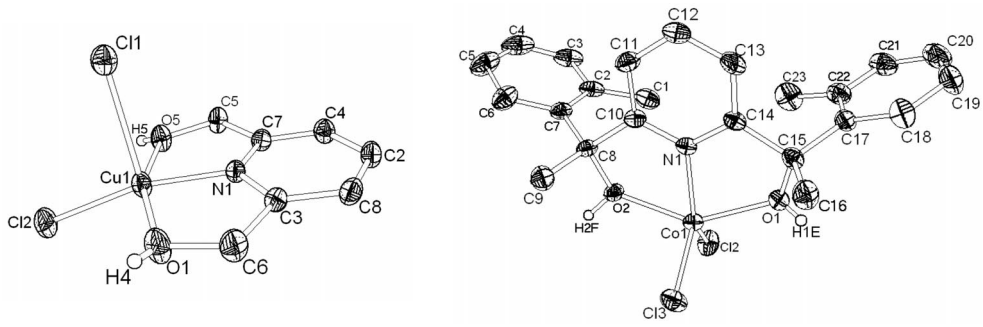

Figure 2. View of the molecular structures of $[(pydimH_2)CuCl_2]\cdot H_2O$ (left) and $[(pydotH_2)CoCl_2]\cdot EtOH$ (right) (thermal ellipsoids represent 30% probability). The H atoms on the ligands' oxido functions are displayed, whereas other H atoms and the ethanol molecule have been omitted for clarity.

Table 1. Selected structural data for complexes of the type $[(RR'pydimH_2)MCl_2]$.

	$[(pydotH_2)ZnCl_2]\cdot$ EtOH	$[(pydimH_2)ZnCl_2]$ in $P2_1/c$	$[(pydimH_2)ZnCl_2]$ in $P\bar{1}$	$[(pydotH_2)CoCl_2]\cdot$ EtOH	$[(pydotH_2)NiCl_2]\cdot$ EtOH	$[(pydimH_2)CuCl_2]\cdot H_2O$
M–N	2.070(3)	2.042(3)	2.037(3)	2.038(2)	1.962(6)	1.929(1)
M–O	2.165(3)	2.222(2)	2.142(4)	2.143(2)	2.074(6)	2.001(2)
	2.153(3)	2.153(2)	2.162(4)	2.132(2)	2.063(6)	1.997(2)
M–Cl	2.257(1)	2.277(1)	2.285(1)	2.283(1)	2.294(2)	2.6960(9)
	2.218(1)	2.233(1)	2.230(1)	2.247(1)	2.242(2)	2.2076(7)
O–M–O	143.9(2)	151.7(1)	144.6(1)	146.28(8)	150.5(2)	159.16(7)
O–M–N	74.3(1)	75.7(1)	74.9(1)	75.43(9)	77.8(3)	79.24(7)
	74.4(1)	76.1(1)	75.2(1)	75.56(9)	77.5(2)	80.36(6)
Cl–M–Cl	118.32(6)	113.58(4)	110.42(5)	117.24(4)	113.32(9)	101.24(3)
Cl–M–N	106.8(1)	117.77(9)	105.9(1)	105.83(7)	101.6(2)	93.58(5)
	134.8(1)	128.58(9)	143.7(1)	136.89(7)	145.1(2)	165.16(5)
NOOM/ ClClM	90.6(1)	90.6(1)	88.5(1)	90.5(1)	89.5(1)	93.0(1)

gen-bonding interactions are also observed here. The shortest are found between the carboxylate anions and the H–O function in $[(pydimH_2)_2Co][TFA]_2$, where the O···H distance of 1.674(5) Å [O···O 2.577(6) Å] and the O–H···O angle of 172.9(5)° classify them as medium to strong H bonds.[27] The metal centres in the dicationic complexes are coordinated by two RR′pydim ligands in an approximately octahedral environment. Table 4 lists selected bond lengths and angles.

At first sight, the bond lengths and angles around the metal atoms are quite similar in all the structures, and the two pyridine rings are oriented almost perpendicular to each other. However, a closer look reveals differences between the structures of the Co and Zn derivatives and that of the Cu complex. For example, the four oxido donor atoms are not arranged in a square-planar fashion due to the geometrical restriction enforced by the pincer ligand. The deviation of the square plane towards a tetrahedron can best be described by the sum of the angles around the metal atom, which is about 305° for the Co and Zn derivatives and thus far from the required 360° for a perfect plane. The corresponding value for the Cu derivative is 313° (Table 4). The most striking finding are the bond lengths in the Cu complex $[(pydipH_2)_2Cu]Cl_2\cdot H_2O$. The two axial N–M bonds are markedly shorter than the equatorial M–O bonds, which is the opposite of what would have been expected from a normal Jahn–Teller distortion. Our series of

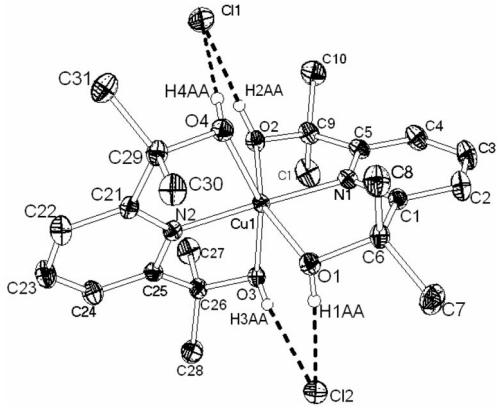

Figure 3. View of the molecular structure of $[(pydipH_2)_2Cu]Cl_2\cdot H_2O$ (thermal ellipsoids represent 30% probability). The H atoms on the ligands' oxido functions are displayed, whereas other H atoms and the water molecule have been omitted for clarity. Shortest H···Cl contact: Cl(1)···H(2) [2.156(7) Å]; Cl(1)···O(2) 3.055(5) Å; angle O–H···Cl 170.9(5)°.

complexes also reveals that the M–N distances are shorter for the Cu^{II} derivative than for the Co or Zn analogues and that the four (equatorial) M–O bonds in the copper complex are slightly longer than those of the Co or Zn derivatives. We therefore assume a tetragonal compressive effect

for this complex. This is in line with the Jahn–Teller theorem, which includes both tetragonal compressions or extensions.[28,29]

Weber et al. have recently investigated the crystal structures of complexes with $pydimH_2$ and Co, Ni and Cu.[14] The complexes $[(pydimH_2)_2Co]^{2+}$ with various anions such as NO_3^-, SO_4^{2-} or *p*-$TolOSO_3^-$ exhibit very similar structural parameters when compared with our $pydimH_2$ and $pydipH_2$ derivatives.[14a] Interestingly, a complex $[(pydimH_2)(pydimH)Co^{III}]Cl_2$ was obtained, in which deprotonation of the ligand occurs concomitantly with oxidation of the central metal atom (Co^{II} to Co^{III}). Similarly, a Cu^{II} complex containing a partially deprotonated ligand – $[(pydimH_2)(pydimH)Cu]ClO_4$ – was reported.[14b] In both cases the corresponding M–O bonds are about 10% shorter than the corresponding bonds with protonated O atoms (M–OH). Four further copper complexes $[(pydimH_2)_2Cu]^{2+}$ have been crystallised with structural parameters very similar to our structure with the $pydipH_2$ ligand. The axial N–Cu bonds are also rather short in this complex, with values ranging from 1.935(4) Å to 2.102(3) Å, clearly indicating a Jahn–Teller-like compression.[14b] A number of nickel complexes $[(pydimH_2)_2Ni]^{2+}$ with various counterions (Cl^-, NO_3^-, SO_4^{2-}, *p*-$TolOSO_3^-$) have also been reported. These complexes also show shortened axial M–N distances of about 1.97 Å, whereas the equatorial M–O(H) bonds lie in the same range as those of Ni and Cu derivatives (about 2.1 Å).[14a] Unfortunately, we were not able to include the crystal structure of a nickel derivative in our series, but we are quite confident that its structural parameters would be quite similar.

A third type of structure is represented by the complex *trans*-$[(pydimH_2)_2PdCl_2]\cdot 2H_2O$ (data collected in Table 5), which is isostructural with the already reported Pt^{II} derivative.[24] The two $pydimH_2$ ligands bind to the metal atom through their pyridine donor function, and the OH group is bent away. There are medium-strong hydrogen-bonding interactions between the OH group and the co-crystallised water molecules, with an O···H distance of 2.225(5) Å [O···O 2.780(4) Å] and an O–H···O angle of 161.1(6)°. Due to the steric demand of the $pydimH_2$ ligands the complexes are *trans*-configured, although the *cis* configuration would be preferred on electronic grounds.[30] This finding strongly supports the proposal that the failure to form complexes with the bulky ligands $pydipH_2$ and $pydotH_2$ is due to repulsion of the ancillary R′ groups of the bulkier RR′$pydimH_2$ ligands.

The two compounds *cis*- and *trans*-$[(pydimH_2)(dmso)PtCl_2]$ formed from the reaction of the complex precursor $[(dmso)_2PtCl_2]$ with 1 equiv. of $pydimH_2$ were also crystallised and structurally characterised (see, for example Figure 4; crystallographic data listed in Table 5).

The crystal structure of the *cis* derivative shows a short O–H···O contact of 1.943(5) Å [angle: 149.5(4)°; O···O 2.682(4) Å] which can be classified as an H bond of medium strength. The analogous interaction in the *trans* derivative is much weaker [2.108(6) Å; 146.8(4)°; 2.829(4) Å], although neither is likely to have any significant impact on the molecular structures. The coordination geometry around the metal atom is square-planar, as expected, and the bond lengths around the metal atom in the two stereoisomeric Pt complexes show clear trends in terms of the *trans* influence of ligands. For example, the Pt–N bond is slightly shorter in the *cis*-configured Pt derivative, which is in line with dmso being a stronger ligand than Cl. Upon comparing the Pt–S bond lengths, we can see that this bond is shorter in the *cis* derivative than in the *trans* derivative, which means that Cl is a weaker ligand than $pydimH_2$. In summary, the ligands can be sorted into a series with decreasing *trans* influence: dmso > $pydimH_2$ > Cl. The influence of the $pydimH_2$ ligand is very similar to the well-known ligand 1,4-pyrazine (pyz) in the dinuclear complexes *trans*-[(μ-pyz){$(R_2SO)PtCl_2$}$_2$] (R = *n*Bu, *n*Pr or *c*Bu), which show Pt–S bond lengths of about 2.222(2) Å.[31] From the series of ligand strengths, we assume that the *cis* isomer of $[(pydimH_2)(dmso)PtCl_2]$ is thermodynamically favoured, and the *trans* isomer is presumably the kinetic product. The latter finding leads to the assumption of an associative ligand-exchange reaction through a five-coordinate transition state (or intermediate).[30,32] This, and its superior solubility, enabled us to isolate it. This is important since the two complexes are interesting candidates as building blocks for di- or oligonuclear (heterometallic) complexes, as the dmso ligand can easily be replaced by other ligands. Future work will be devoted to this subject.

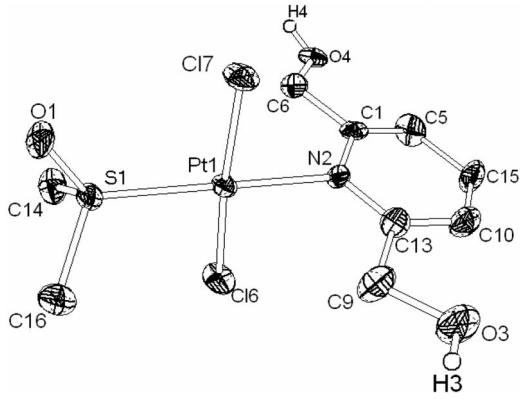

Figure 4. View of the molecular structure of *trans*-$[(pydimH_2)(dmso)PtCl_2]$ (thermal ellipsoids represent 30% probability). The H atoms on the ligand's oxido functions are displayed, whereas other H atoms have been omitted for clarity.

Molecular Structures of the Complexes in Solution

NMR Spectroscopy

Unfortunately, no NMR spectra could be obtained for most of the complexes due to their paramagnetism (Co^{II}, Ni^{II}, Cu^{II}). A largely broadened ^1H NMR spectrum is observed for $[(pydotH_2)_2NiCl_2]$ (see the Supporting Information), and we therefore assume a high-spin configuration for this complex. The Zn^{II} complexes generally gave good NMR spectra in [D$_6$]acetone solution, and selected reso-

Table 2. Selected NMR spectroscopic data for the oxido pincer ligands and their Zn^{II} complexes.[a]

Compound	^{1}H			^{13}C		
	4-Py	3,5-Py	OH	4-Py	2,6-Py	C(OH)
pydimH_2	7.77	7.34	4.43	136.8	160.3	64.3
[(pydimH_2)$ZnCl_2$]	7.98	7.46	_[b]	_[c]	_[c]	_[c]
pydipH_2	7.72	7.32	4.16	137.6	165.8	72.3
[(pydipH_2)$_2$Zn]$^{2+}$	8.19	7.74	6.94	141.4	162.8	72.8
pydot$H_2^{R,S}$	7.62	7.02	5.44	137.6[d]	164.4[d]	76.3[d]
pydot$H_2^{R,R}$	7.63	7.07	5.39	137.6[d]	164.4[d]	76.3[d]
[(pydot$H_2^{R,S}$)$ZnCl_2$]	7.89	6.97	7.67	141.4[d]	162.8[d]	76.7[d]
[(pydot$H_2^{R,R}$)$ZnCl_2$]	7.89	6.96	7.54	141.4[d]	162.8[d]	76.7[d]

[a] Chemical shifts (δ) in ppm, as measured in [D_6]acetone. [b] Not observed due to broadening. [c] Not observed due to low solubility. [d] Isomers could not be assigned separately.

nances are summarised together with those of the free ligands in Table 2 (see the Experimental Section for complete data).

It is evident from Table 2 that coordination of the metal ions leads to a general shift to lower field for the ^{1}H and ^{13}C resonances. The spectra were found to be unchanged even after one week in the corresponding solvent, thereby proving the stable coordination of the ligands. Several sets of signals were observed for the chiral ligand pydotH_2 and its Zn complex, and we were able to assign these to the (*R*,*S*) or (*R*,*R*) enantiomers (see Table 2).

The NMR spectra of both crude and recrystallised [(pydimH_2)$_2$$PtCl_2$] point to the exclusive *trans* configuration of this complex,[24] whereas a 1:1 mixture of *cis*/*trans* isomers was observed for [(pydimH_2)(dmso)$PtCl_2$]. The $^3J_{H_{(dmso)},Pt}$ coupling is slightly larger for the *cis* complex (24.1 Hz), than for the *trans* derivative (20.9 Hz), which suggests that the pydimH_2 ligand possesses a slightly larger *trans* influence than the chlorido ligand. We can also conclude that the bulkiness of the ancillary R and R′ groups of the RR′pydimH_2 ligands has a strong impact on the observed stereochemistry and very probably inhibits complex formation for the more bulky ligands pydipH_2 and pydotH_2. A *trans* configuration is assumed for the palladium complex [(pydimH_2)$_2$$PdCl_2$] from the very high similarity of the ^{1}H shifts with those of the platinum analogue.

Optical Spectroscopy of the Complexes in Solution

Since NMR spectroscopy could not provide evidence for stable coordination in solution for the majority of our complexes, absorption spectra were recorded for selected examples. Bands in the UV spectrum at around 270 nm (λ_1) were observed for all compounds. These bands are typical for 2,6-disubstituted pyridine ligands (π-π* transitions), and discrimination between coordinated and free ligands on this basis is not feasible. The Zn^{II} complexes do not exhibit any further absorption bands, whereas the Co, Ni, Co, Pd, and Pt complexes show additional bands arising from the metal atoms. For the 3d elements Co, Ni, and Cu these are typical ligand-field (d-d) transitions, whereas charge-transfer transitions are assumed for the observed long-wavelength absorption bands for Pd and Pt. A table containing all spectroscopic data and assignments is provided in the Supporting Information.

The spectra of most of the octahedrally configured complexes [(RR′pydimH_2)$_2$M]$^{2+}$ (M = Co, Ni, Cu. Zn) in MeCN solution remain unchanged for several days, thus indicating that these species are configurationally stable in this rather polar solvent. Interestingly, [(pydimH_2)$_2$Ni]Cl_2 is not stable in MeCN solution as the solution immediately turns from light green to intense yellow. The nature of the decomposition product is not yet clear, although it is likely that the oxido pincer ligand is replaced by MeCN molecules. The rather low energy of the ligand-field bands of the pydipH_2 derivative suggests rather weak bonding to Ni^{II}. We assume that for the slightly weaker pydimH_2 ligand MeCN readily replaces the pincer ligand to form species such as [(MeCN)$_6$Ni]$^{2+}$.[33]

When compounds of the type [(RR′pydimH_2)$_2$Co]-[$CoCl_4$] are dissolved in the apolar solvent CH_2Cl_2 the complexes undergo "coordination disproportionation"[34] according to Equation (1).

$$[(RR'pydimH_2)_2M][MCl_4] \rightleftarrows 2\,[(RR'pydimH_2)MCl_2] \quad (1)$$

This fully reversible process is shown for the system [(pydotH_2)$_2$Co][$CoCl_4$] ⇄ 2 [(pydotH_2)$CoCl_2$] in Figure 5. The visible part of the spectrum of the first form (in pure MeCN solution) is dominated by the absorption bands of [$CoCl_4$]$^{2-}$, and the absorptions of the dicationic complex [(pydotH_2)$_2$Co]$^{2+}$ are obscured by this relatively strong absorption. The spectrum of the neutral species [(pydotH_2)-$CoCl_2$] (in pure CH_2Cl_2 solution) consists of a relatively weak structured band with a maximum at 628 nm (15920 cm^{-1}) and shoulders at 587 nm (17030 cm^{-1}) and 400 nm (25000 cm^{-1}). These absorptions are attributed to the $^4A'_2 \rightarrow {}^4A'_2$, $^4A'_2 \rightarrow {}^4E'$, and $^4A'_2 \rightarrow {}^4E''$ transitions in a d^7 high-spin system.[29,35]

The pentacoordinate complexes [(RR′pydimH_2)$CuCl_2$] with pydimH_2 and pydipH_2 undergo disproportionation in MeCN solution to yield the octahedral species [(RR′pydim)$_2$-Cu]$^{2+}$ and [$CuCl_4$]$^{2-}$. However, this disproportionation occurs far slower than for the corresponding Co^{II} systems. The complex ion [$CuCl_4$]$^{2-}$ is clearly characterised by the intense charge-transfer band (LMCT) at 462 nm (21645 cm^{-1}).[36] A high-energy shoulder visible at around 389 nm points to partial solvolysis in MeCN solution to

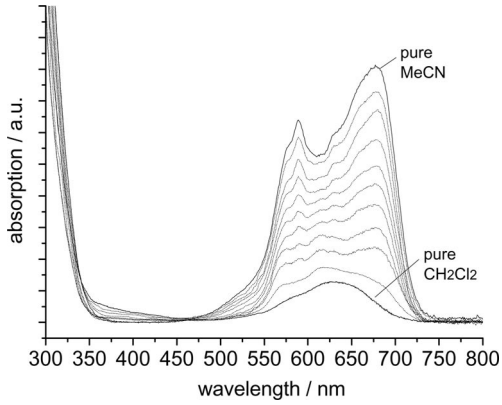

Figure 5. Absorption spectra of the equilibrium $[(pydotH_2)_2Co][CoCl_4] \rightleftarrows 2\ [(pydotH_2)CoCl_2]$ in mixtures of MeCN and CH_2Cl_2. The traces represent mixtures from 10:0 (pure MeCN), 9:1, 8:2 to 1:9 and 0:10 (pure CH_2Cl_2).

give $[CuCl_3(MeCN)]^-$.[36,37] The octahedral species $[(RR'pydim)_2Cu]^{2+}$ shows long-wavelength bands at around 900 nm (11100 cm^{-1}) accompanied by long-wavelength shoulders. These bands can clearly be assigned to the expected Jahn–Teller-distorted ligand-field transition. The nickel complex $[(pydotH_2)NiCl_2]$ exhibits an absorption spectrum typical for a pentacoordinate high-spin d^8 system[29,35] and is completely stable in all solvents.

The spectra of the square-planar Pt^{II} and Pd^{II} complexes $[(pydimH_2)MCl_2]$ look very similar to the spectrum of *trans*-$[(py)_2PtCl_2]$, which confirms that the complex entity is conserved in MeCN solution. Again, no spectral changes were observed after several days.

Conclusion and Outlook

Our study of the coordination chemistry of the three 2,6-bis(hydroxymethyl)pyridine-based oxido pincer ligands $RR'pydimH_2$ [R = R′ = H ($pydimH_2$); R = R′ = Me ($pydipH_2$); R = 2-tolyl, R′ = Me ($pydotH_2$)] with late transition metals Co^{II}, Ni^{II}, Cu^{II}, Zn^{II}, Pd^{II}, and Pt^{II} has revealed a wealth of structural motifs, including square-planar (Pt, Pd), trigonal-bipyramidal (Co, Ni, Zn), square-pyramidal (Cu), and octahedral (Co, Ni, Cu, Zn) coordination. The oxido functions coordinate to the 3d elements with no deprotonation of the OH group but fail to bind to the (very soft) palladium and platinum atoms. The 3d metals form two main complex species, which interconvert upon changing the solvent polarity. Polar solvents promote the formation of the dicationic species $[(RR'pydimH_2)_2M]^{2+}$, whereas apolar solvents favour the neutral complexes $[(RR'pydimH_2)MCl_2]$. Their identity and the equilibrium between the two forms have been established by ^1H NMR spectroscopy for the diamagnetic Zn^{II} complexes and by UV/Vis/NIR spectroscopy for the paramagnetic Co^{II}, Ni^{II}, and Cu^{II} derivatives. Pd^{II} and Pt^{II} form square-planar complexes of the type *trans*-$[(pydimH_2)_2MCl_2]$. The complexes $[(pydimH_2)(dmso)MCl_2]$ form *cis* and *trans* isomers (ratio ca. 1:1). These findings emphasize the relative bulkiness of the oxido pincer ligands and explain the failure of the bulkier ligands $pydipH_2$ or $pydotH_2$ to coordinate to the two platinum metals.

Future work will focus on the development of further oxido pincer ligands of the type RR′pydim with a strong emphasis on chiral derivatives. The use of deprotonated ligands or the deprotonation reaction "on site" will also be studied. An interesting aspect in this respect is the coupling of the protonation/deprotonation with changes in the redox state. Generally, our expectation that the pyridine function will reliably bind to the metal atom and that the oxido functions are much more weakly bound is largely fulfilled for the series of complexes presented herein. The reactivity patterns of these complexes that are expected to arise from these weak interactions, for example C–H or C–X activation, will also be studied in the future in the light of catalytic applications.

Experimental Section

General: Dimethyl pyridine-2,6-dicarboxylate, 2,6-diacetylpyridine, 2,6-bis(hydroxymethyl)pyridine, and MeLi were purchased from Aldrich. All reactions were carried out under inert-gas conditions by using Schlenk techniques. Solvents (CH_2Cl_2, thf, toluene, Et_2O, and MeCN) were dried by using an MBRAUN MB SPS-800 solvent purification system.

Instrumentation: NMR spectra were recorded with a Bruker Avance II 300 MHz spectrometer by using a triple-resonance ^1H, ^{n}BB inverse probe head. Unambiguous assignment of the ^1H and ^{13}C resonances was achieved from ^1H TOCSY, ^1H COSY, gradient-selected ^1H, ^{13}C HSQC, and HMBC spectra. All 2D NMR experiments were performed by using standard pulse sequences from the Bruker pulse program library. Chemical shifts are quoted relative to TMS. UV/Vis/NIR absorption spectra were measured with a Varian Cary50 Scan or Shimadzu UV-3600 photospectrometer. Elemental analyses were performed by using a HEKAtech CHNS EuroEA 3000 Analyzer.

Synthesis of the Oxido Pincer Ligands

2,6-Bis(1-hydroxy-1-methylethyl)pyridine ($pydipH_2$): This ligand was synthesised according to a modified literature procedure.[26] Thus, MeLi (54 mL of a 1.6 M solution, 86 mmol) was added dropwise to dimethyl pyridine-2,6-dicarboxylate (4 g, 20.05 mmol) in thf (100 mL) at –78 °C. After stirring at room temperature for 2 h, the mixture was quenched with an aqueous saturated NH_4Cl solution (100 mL) and extracted with CH_2Cl_2 (5 × 30 mL). The dark oil obtained upon evaporation of the CH_2Cl_2 extracts was purified by chromatography on silica gel by using cyclohexane/ethyl acetate (5:1) to give an orange oil. This oil was finally crystallised from an acetone/pentane mixture (1:1) at 0 °C to give colourless crystals. Yield: 2.74 g (70%). ^1H NMR (300 MHz, $CDCl_3$): δ = 7.72 (t, J = 7.79 Hz, 1 H, 4-Py), 7.32 (d, J = 7.79 Hz, 2 H, 3,5-Py), 4.16 (m, 2 H, OH), 1.57 (s, 12 H, CH_3) ppm. ^{13}C NMR (75 MHz, [D_6]acetone): δ = 165.8 (2 C, 2,6-Py), 137.6 (1 C, 4-Py), 116.5 (2 C, 3,5-Py), 72.3 [2 C, C(OH)], 30.1 (4 C, CH_3) ppm. $C_{11}H_{17}NO_2$ (195.26): calcd. C 67.66, H 8.78, N 7.17; found C 67.51, H 8.80, N 7.16.

2,6-Bis(1-hydroxy-1-*o*-tolylethyl)pyridine ($pydotH_2$): A freshly prepared solution of *o*-tolylmagnesium bromide (20.4 mmol) in Et_2O (20 mL) was added dropwise to 2,6-diacetylpyridine (1632 mg, 10 mmol) in Et_2O (50 mL) at 0 °C. The reaction mixture was stirred

overnight and then quenched with an aqueous saturated NH_4Cl solution (50 mL). After extraction with CH_2Cl_2 (3 × 30 mL) and evaporation of the organic solvents, the product was recrystallized as a colourless solid from ethanol/water (1:2). Yield: 1.56 g (45%). ^{1}H NMR (300 MHz, [D$_6$]acetone): (*R*,*R*/*S*,*S*) isomer: δ = 7.69 (dd, J_1 = 7.30, J_2 = 1.90 Hz, 2 H, 6-Tol), 7.62 (t, J = 7.76 Hz, 1 H, 4-Py), 7.13–7.25 (m, 4 H, 4,5-Tol), 7.07 (m, 2 H, 3-Tol), 7.02 (m, 2 H, 3,5-Py), 5.39 (s, 2 H, OH), 1.95 (s, 6 H, C*H*$_3$Tol), 1.88 (s, 6 H, CH_3) ppm; (*R*,*S*/*S*,*R*) isomer: δ = 7.69 (dd, J_1 = 7.30, J_2 = 1.90 Hz, 2 H, 6-Tol), 7.63 (t, J = 7.74 Hz, 1 H, 4-Py), 7.13–7.25 (m, 4 H, 4,5-Tol), 7.07 (d, J = 7.21 Hz, 2 H, 3-Tol), 7.02 (d, J = 7.74 Hz, 2 H, 3,5-Py), 5.44 (s, 2 H, OH), 1.95 (s, 6 H, C*H*$_3$Tol), 1.86 (s, 6 H, CH_3) ppm. ^{13}C NMR (75 MHz, [D$_6$]acetone): δ = 164.4 (2 C, 2,6-Py), 144.0 (2 C, 1-Tol), 137.6 (1 C, 4-Py), 131.9 (2 C, 5-Tol), 127.4 (2 C, 4-Tol), 126.5 (2 C, 2-Tol), 125.2 (2 C, 3-Tol), 125.1 (2 C, 6-Tol), 118.1 (2 C, 3,5-Py), 76.3 [2 C, *C*(OH)], 30.9 (2 C, CH_3), 20.6 (2 C, *C*H$_3$Tol) ppm (isomers not assigned). $C_{23}H_{25}NO_2$ (347.5): calcd. C 79.51, H 7.25, N 4.03; found C 77.36, H 7.47, N 4.06.

General Procedure for Complex Synthesis: In a typical reaction, the ligand (1 mmol) was dissolved in ethanol (5 mL) and subsequently added dropwise to a solution of the corresponding M^{II} salt (1 mmol) in ethanol (10–15 mL). The mixture was stirred at room temperature overnight, then the solvent was removed under reduced pressure and the residue recrystallized three times from acetone and pentane to afford the coloured products.

[(pydimH$_2$)$_2$Co][CoCl$_4$]: Synthesized from $CoCl_2·6H_2O$ and pydimH$_2$ in a 1:1 ratio and isolated as blue crystals. Yield: 269 mg (50%). $C_{14}H_{18}Cl_4Co_2N_2O_4$ (537.98): calcd. C 31.26, H 3.37, N 5.21; found C 31.27, H 3.36, N 5.18.

[(pydimH$_2$)$_2$Co][TFA]$_2$: $CoCl_2·6H_2O$ (238 mg, 1.00 mmol) and pydimH$_2$ (290 mg, 2.08 mmol) were stirred in trifluoroacetic acid (10 mL) overnight. The solvent was evaporated and the resulting oily purple crude product stored at 0 °C. After 3 weeks, purple crystals were collected and washed three times with cold ethanol. Yield: 201 mg (36%). $C_{18}H_{18}CoF_6N_2O_8$ (563.27): calcd. C 38.38, H 3.22, N 4.97; found C 39.01, H 3.12, N 4.85.

[(pydimH$_2$)NiCl$_2$]: Synthesized from anhydrous $NiCl_2$ and pydimH$_2$ and isolated as a bright green powder. Yield: 234 mg (87%). $C_7H_9Cl_2NNiO_2$ (268.75): calcd. C 31.28, H 3.38, N 5.21; found C 30.35, H 3.26, N 5.12.

[(pydimH$_2$)CuCl$_2$]: Synthesized from $CuCl_2·3H_2O$ and pydimH$_2$ and isolated as turquoise crystals. Yield: 175 mg (64%). $C_7H_9Cl_2CuNO_2$ (273.60): calcd. C 30.73, H 3.32, N 5.12; found C 30.76, H 3.30, N 5.13.

[(pydimH$_2$)ZnCl$_2$]: Synthesized from $ZnCl_2·2H_2O$ and pydimH$_2$ and isolated as a colourless solid. Yield: 203 mg (74%). ^{1}H NMR (300 MHz, [D$_6$]acetone + some drops of water): δ = 7.98 (t, J = 7.80 Hz, 1 H, 4-Py), 7.46 (d, J = 7.80 Hz, 2 H, 3,5-Py), 4.87 (s, 4 H, C*H*$_2$OH) ppm; signals for OH were not found. No ^{13}C NMR spectrum could be obtained due to low solubility in common organic solvents. $C_7H_9Cl_2NO_2Zn$ (275.45): calcd. C 30.52, H 3.29, N 5.09; found C 30.09, H 3.25, N 4.89.

[(pydimH$_2$)$_2$PdCl$_2$]: pydimH$_2$ (140 mg, 1.0 mmol) was dissolved in acetone (10 mL) and added dropwise to an aqueous solution (2 mL H_2O) of $K_2[PdCl_4]$ (326 mg, 1.0 mmol). The mixture was stirred at room temperature for 1 h, then all volatiles were removed. The light-yellow product was extracted from the residue with CH_2Cl_2. Yield: 160 mg (36%). ^{1}H NMR (300 MHz, [D$_6$]acetone): δ = 8.03 (t, J = 7.78 Hz, 1 H, 4-Py), 7.70 (d, J = 7.78 Hz, 2 H, 3,5-Py), 6.05 (d, J = 5.51 Hz, 4 H, C*H*$_2$OH), 5.20 (t, J = 5.51 Hz, 2 H, OH) ppm. ^{13}C NMR (75 MHz, [D$_6$]acetone): δ = 163.5 (2 C, 2,6-Py), 139.6 (1 C, 4-Py), 120.8 (2 C, 3,5-Py), 64.9 [2 C, C(OH)] ppm. $C_{14}H_{18}Cl_2N_2O_4Pd$ (455.63): calcd. C 36.90, H 3.98, N 6.15; found C 36.91, H 3.98, N 6.13.

[(pydimH$_2$)$_2$PtCl$_2$]: pydimH$_2$ (140 mg, 1.0 mmol) was dissolved in acetone (10 mL) and added dropwise to an aqueous solution (2 mL H_2O) of $K_2[PtCl_4]$ (206 mg, 0.5 mmol). After stirring of the reaction mixture at room temperature for 2 h, all volatiles were distilled off with a rotary evaporator at 65 °C. The residue was extracted three times with an acetone/pentane mixture (3:1) (30 mL) to give a light yellow product upon evaporation of the remaining solvent. Yield: 405 mg (77%). ^{1}H NMR (300 MHz, [D$_6$]acetone): δ = 8.17 (t, J = 7.50 Hz, 2 H, 4-Py), 7.67 (d, J = 7.50 Hz, 4 H, 3,5-Py), 5.85 (br. s, 8H CH_2), 4.85 (br. s, 4 H, OH) ppm. ^{13}C NMR (75 MHz, [D$_6$]acetone): δ = 164.1 (4 C, 2,6-Py), 139.6 (2 C, 4-Py), 120.8 (4 C, 3,5-Py), 63.8 (4 C, CH_2) ppm. No satellites due to coupling to ^{195}Pt were observed.

[(pydipH$_2$)$_2$Co][CoCl$_4$]: Synthesized from $CoCl_2·6H_2O$ and pydipH$_2$ and isolated as blue crystals. Yield: 377 mg (58%). $C_{22}H_{34}Cl_4Co_2N_2O_4$ (650.19): calcd. C 40.64, H 5.27, N 4.31; found C 40.85, H 5.35, N 4.32.

[(pydipH$_2$)$_2$Ni]Cl$_2$: Synthesized from anhydrous $NiCl_2$ and pydipH$_2$ (2 equiv.) and isolated as a turquoise solid. Yield: 359 mg (69%). $C_{22}H_{34}Cl_2N_2NiO_4$ (520.12): calcd. C 50.80, H 6.59, N 5.39; found C 50.78, H 6.61, N 5.35.

[(pydipH$_2$)CuCl$_2$]: Synthesized from $CuCl_2·2H_2O$ and pydipH$_2$ and isolated as a blue powder. Yield: 310 mg (94%). $C_{11}H_{17}Cl_2CuNO_2$ (329.71): calcd. C 40.07, H 5.20, N 4.25; found C 40.62, H 5.40, N 4.13.

[(pydipH$_2$)$_2$Cu]Cl$_2$: Synthesized from $CuCl_2·2H_2O$ and pydipH$_2$ (2 equiv.) and isolated as a turquoise powder. Yield: 521 mg (96%). $C_{22}H_{36}Cl_2CuN_2O_5$ (542.98): calcd. C 47.66, H 6.68, N 5.16; found C 47.05, H 6.55, N 5.02.

[(pydipH$_2$)$_2$Zn][ZnCl$_4$]: Synthesized from $ZnCl_2·2H_2O$ and pydipH$_2$ and isolated as colourless to yellowish fine needles. Yield: 557 mg (84%). ^{1}H NMR (300 MHz, [D$_6$]acetone): δ = 8.19 (t, J = 7.95 Hz, 1 H, 4-Py), 7.74 (d, J = 7.95 Hz, 2 H, 3,5-Py), 6.94 (s, 1 H, OH), 1.78 (s, 12 H, CH_3) ppm. ^{13}C NMR (75 MHz, [D$_6$]acetone): δ = 162.8 (2 C, 1-Py), 141.4 (1 C, 4-Py), 119.5 (2 C, 3,5-Py), 72.8 [2 C, C(OH)], 29.9 (2 C, CH_3) ppm. $C_{22}H_{34}Cl_4N_2O_4Zn_2$ (663.11): calcd. C 39.85, H 5.17, N 4.22; found C 38.45, H 5.09, N 4.11.

[(pydotH$_2$)CoCl$_2$]·EtOH: Synthesized from $CoCl_2·6H_2O$ and pydotH$_2$ and isolated as blue crystals. Yield: 261 mg (50%). $C_{25}H_{31}Cl_2CoNO_3$ (523.36): calcd. C 57.37, H 5.97, N 2.68; found C 56.59, H 5.89, N 2.58.

[(pydotH$_2$)NiCl$_2$]·EtOH: Addition of pydotH$_2$ to a solution of anhydrous $NiCl_2$ immediately led to a pink solution. The usual workup afforded a pink powder. Yield: 355 mg (68%). $C_{25}H_{31}Cl_2NNiO_3$ (523.12): calcd. C 57.40, H 5.97, N 2.68; found C 57.45, H 6.23, N 2.64.

[(pydotH$_2$)CuCl$_2$]·EtOH: Synthesized from $CuCl_2·2H_2O$ and pydotH$_2$ and isolated as a green solid. Yield: 177 mg (55%). $C_{25}H_{31}Cl_2CuNO_3$ (527.98): calcd. C 56.87, H 5.92, N 2.65; found C 56.16, H 5.84, N 2.67.

[(pydotH$_2$)ZnCl$_2$]·EtOH: Synthesized from $ZnCl_2·2H_2O$ and pydotH$_2$ and isolated as a colourless solid. Yield: 493 mg (93%). ^{1}H NMR (300 MHz, [D$_6$]acetone): (*R*,*S*/*S*,*R*) isomer (77%): δ = 7.89 (t, J = 7.86 Hz, 1 H, 4-Py), 7.81 (m, 2 H, 6-Tol), 7.67 (s, 2 H, OH), 7.32 (m, 2 H, 5-Tol), 7.21 (m, 2 H, 4-Tol), 7.18 (m, 2 H, 3-Tol), 6.97 (d, J = 7.86 Hz, 2 H, 3,5-Py), 2.21 (s, 6 H, CH_3), 2.06 (s, 6 H, CH_3Tol) ppm; (*S*,*S*/*R*,*R*) isomer (23%): δ = 7.89 (t, J =

7.86 Hz, 1 H, 4-Py), 7.81 (m, 2 H, 6-Tol), 7.54 (s, 2 H, OH), 7.32 (m, 2 H, 5-Tol), 7.21 (m, 2 H, 4-Tol), 7.18 (m, 2 H, 3-Tol), 6.96 (d, J = 7.86 Hz, 2 H, 3,5-Py), 2.06 (s, 6 H, CH_3Tol), 2.00 (s, 6 H, CH_3) ppm. ^{13}C NMR (75 MHz, [D$_6$]acetone): δ = 162.8 (2 C, 2,6-Py), 141.4 (1 C, 4-Py), 138.2 (2 C, 1-Tol), 132.4 (2 C, 5-Tol), 128.8 (2 C, 4-Tol), 126.9 (2 C, 2-Tol), 125.5 (2 C, 6-Tol), 125.5 (2 C, 3-Tol), 120.2 (2 C, 3,5-Py), 76.7 [2 C, C(OH)], 30.1 (2 C, CH_3), 21.0 (2 C, CH_3Tol) ppm. $C_{25}H_{31}Cl_2NO_3Zn$ (529.81): calcd. C 56.67, H 5.90, N 2.64; found C 56.65, H 5.80, N 2.59.

Alternative Synthesis of [(pydimH_2)$_2$PdCl$_2$]: pydimH_2 (140 mg, 1.0 mmol) was dissolved in CH_2Cl_2 (10 mL) and added dropwise to a solution of [(dmso)$_2$PdCl$_2$] (333 mg, 1.0 mmol) in CH_2Cl_2 (25 mL). A yellow precipitate formed after 15 min, and the reaction was finished after 20 min. The solvent was then evaporated to around half of the original volume and the precipitate washed several times with small portions of CH_2Cl_2 and pentane to yield a light yellow solid. Yield: 217 mg (48%). ^{1}H, ^{13}C NMR spectroscopic data and elemental analysis were identical to those obtained for the material of the original synthesis method (see above).

***cis*/*trans*-[(pydimH_2)(dmso)PtCl$_2$]:** pydimH_2 (210 mg, 1.5 mmol) was dissolved in CH_2Cl_2 (20 mL) and added dropwise to a solution of [(dmso)$_2$PdCl$_2$] (500 mg, 1.5 mmol) in CH_2Cl_2 (50 mL). The mixture was refluxed at 50 °C for about 55 h. The white precipitate formed was filtered off and washed three times with small portions of warm CH_2Cl_2. The yellow filtrate was concentrated to around half of the original volume, and a yellow solid was precipitated by adding pentane. Alternatively, the yellow material can be extracted with Et_2O, as the white solid is not soluble in that solvent. Yield: 360 mg (50% white = *cis* product), 205 mg (28% yellow = *trans* product). ^{1}H NMR (300 MHz, [D$_6$]acetone): *cis* product: δ = 8.10 (t, J = 7.81 Hz, 1 H, 4-Py), 7.74 (d, J = 7.81 Hz, 2 H, 3,5-Py), 5.53 (d, J = 5.51 Hz, 4 H, CH_2), 5.11 (t, J = 5.85 Hz, 2 H, OH), 3.52 [t, $J_{Pt,H}$ = 24.14 Hz, 6 H, CH_3 (dmso)] ppm. ^{13}C NMR (75 MHz, [D$_6$]acetone): *cis* product: δ = 162.9 (2 C, 2,6-Py), 140.0 (1 C, 4-Py), 122.0 (t, $J_{Pt,C}$ = 24.5 Hz, 2 C, 3,5-Py), 63.8 [t, $J_{Pt,C}$ = 28.0 Hz, 2 C, C(OH)], 42.3 [t, J = 57.5 Hz, 2 C, CH_3 (dmso)] ppm. ^{1}H NMR (300 MHz, [D$_6$]acetone): *trans* product: δ = 8.11 (t, J = 7.76 Hz, 1 H, 4-Py), 7.77 (d, J = 7.76 Hz, 2 H, 3,5-Py), 5.55 (d, J = 5.49 Hz, 4 H, CH_2), 5.04 (t, J = 5.96 Hz, 2 H, OH), 3.45 [t, $J_{Pt,H}$ = 20.9 Hz, 6 H, CH_3 (dmso)] ppm. ^{13}C NMR (75 MHz, [D$_6$]acetone): *trans* product: δ = 163.0 (2 C, 2,6-Py), 140.3 (1 C, 4-Py), 122.1 (t, $J_{Pt,C}$ = 34.7 Hz, 2 C, 3,5-Py), 65.2 (t, $J_{Pt,C}$ = 38.6 Hz, 2 C, CH_2), 43.9 [t, $J_{Pt,C}$ = 61.1 Hz, 2 C, CH_3 (dmso)] ppm. $C_9H_{15}Cl_2NO_3PtS$ (483.27): calcd. C 22.37, H 3.13, N 2.90, S 6.64; found C 22.45, H 3.15, N 2.91, S 6.80.

pydipH_2·HCl: The synthesis of pydipH_2·HCl was originally intended as a further purification of the pydipH_2 ligand. Thus, HCl gas (generated from concentrated sulfuric acid and sodium chloride) was slowly added to an Et_2O solution of the ligand pydipH_2 in an open flask equipped with a stirring bar. The reaction was complete when the formation of a white precipitate had finished. The white solid was washed several times with small portions of Et_2O and dried. ^{1}H NMR (300 MHz, [D$_6$]acetone): δ = 7.95 (d, J = 7.77 Hz, 1 H, 5-Py), 7.86 (t, J = 7.77 Hz, 1 H, 4-Py), 7.59 (d, J = 7.77 Hz, 1 H, 3-Py), 4.70 (s, 1 H, OH), 4.20 (s, 1 H, OH′), 1.58 (s, 6 H, CH_3), 1.56 (s, 6 H, CH_3′) ppm. $C_{11}H_{18}ClNO_2$ (231.72): calcd. C 57.02, H 7.83, N 6.04; found C 57.14, H 7.89, N 6.03.

[pydipH_3]$_2$[CoCl$_4$]: Synthesized from $CoCl_2$·6H_2O (119 mg, 0.5 mmol) and pydipH_2·HCl (2 equiv., 196.5 mg, 1.00 mmol) and isolated as light blue crystals. Yield: 152 mg (51%). $C_{22}H_{36}Cl_4CoN_2O_4$ (593.28): calcd. C 44.54, H 6.12, N 4.72; found C 44.14, H 5.99, N 4.73.

X-ray Crystallographic Studies: Crystal structure determinations were performed at 293(2) K by using graphite-monochromated Mo-K_α radiation (λ = 0.71073 Å) with a IPDS II (STOE and Cie.) diffractometer. The structures were solved by direct methods for the free ligand pydotH_2 or by using the Patterson method for all complexes (SHELXS-97)[38] and refined by full-matrix least-squares techniques against F^2 (SHELXL-97).[39] Numerical absorp-

Table 3. Crystal structure and refinement data of complexes [(RR′pydimH_2)MCl$_2$].

Compound	[(pydimH_2)ZnCl$_2$][a]	[(pydimH_2)CuCl$_2$]·H_2O	[(pydotH_2)CoCl$_2$]·EtOH	[(pydotH_2)NiCl$_2$]·EtOH	[(pydotH_2)ZnCl$_2$]·EtOH
Empirical formula	$C_7H_9Cl_2NO_2Zn$	$C_7H_{11}Cl_2CuNO_3$	$C_{25}H_{31}Cl_2CoNO_3$	$C_{25}H_{31}Cl_2NiNO_3$	$C_{25}H_{31}Cl_2NO_3Zn$
Formula mass	275.45	291.62	523.36	523.12	529.81
Crystal system	monoclinic	triclinic	triclinic	triclinic	triclinic
Space group	$P2_1/c$ (No. 14)	$P\bar{1}$ (No. 2)	$P\bar{1}$ (No. 2)	$P\bar{1}$ (No. 2)	$P\bar{1}$ (No. 2)
a [Å]	10.5505(10)	7.3053(15)	10.8545(16)	10.795(2)	10.8962(16)
b [Å]	10.5893(10)	8.0944(16)	10.9814(18)	10.898(2)	10.9913(16)
c [Å]	10.7490(9)	9.8959(19)	11.595(2)	11.476(3)	11.5914(19)
α [°]	90	99.439(16)	87.35(2)	87.36(3)	87.058(19)
β [°]	119.391(4)	109.502(15)	71.492(18)	72.09(3)	71.406(18)
γ [°]	90	96.265(16)	81.867(18)	82.10(2)	81.799(17)
Volume [Å^3], Z	1046.34(17), 1	535.61(18), 2	1297.4(4), 2	1272.4 (5), 2	1302.3(3), 2
F(000)	552	294	546	548	552
Reflections collected	14678	8721	5843	15575	15629
Data/restraints/parameters	2915/0/121	2948/0/144	5843/0/304	5751/2/304	5809/0/299
Goof on F^2	1.334	1.300	0.535	0.569	0.814
Final R indices	R_1 = 0.049,	R_1 = 0.032,	R_1 = 0.033,	R_1 = 0.054,	R_1 = 0.055,
[$I > 2\sigma(I)$]	wR_2 = 0.135	wR_2 = 0.097	wR_2 = 0.057	wR_2 = 0.077	wR_2 = 0.111
R indices	R_1 = 0.057,	R_1 = 0.036,	R_1 = 0.121,	R_1 = 0.252,	R_1 = 0.125,
(all data)	wR_2 = 0.142	wR_2 = 0.094	wR_2 = 0.057	wR_2 = 0.120	wR_2 = 0.126
Largest difference peak/hole [e Å^{-3}]	0.793/–0.701	0.590/–0.481	0.272/–0.245	0.434/–0.357	0.842/–0.598
CCDC-	701771	701773	701780	701781	701782

[a] Another crystalline fraction of the compound was solved in triclinic $P\bar{1}$, the results of the crystal structure refinement were of comparable quality, the data has been deposited with The Cambridge Crystallographic Data Centre (CCDC-701772).

Table 4. Crystal and refinement data and selected bond lengths [Å] and angles [°] for complexes of the type $[(RR'pydimH_2)_2M][X]_2$.

Compound	$[(pydimH_2)_2Co]$-$[TFA]_2$	$[(pydimH_2)_2Co][CoCl_4]\cdot 5/4H_2O$	$[(pydipH_2)_2Co]$-$[CoCl_4]$	$[(pydipH_2)_2Cu]$-$Cl_2\cdot H_2O$	$[(pydipH_2)_2Zn]$-$[ZnCl_4]$
Empirical formula	$C_{18}H_{18}CoF_6N_2O_8$	$C_{14}H_{18}Cl_4Co_2N_2O_4\cdot 5/4\ H_2O$	$C_{22}H_{34}Cl_4Co_2N_2O_4$	$C_{22}H_{36}Cl_2CuN_2O_5$	$C_{22}H_{34}Cl_4Zn_2N_2O_4$
Formula mass	563.27	560.48	650.19	542.98	663.11
Crystal system	triclinic	monoclinic	monoclinic	monoclinic	monoclinic
Space group	$P\bar{1}$ (No. 2)	$P2_1/c$ (No. 14)	$C2/c$ (No. 15)	$P2/c$ (No. 13)	$P2/c$ (No. 13)
a [Å]	7.4407(10)	11.0149(16)	17.474(4)	9.1291(18)	17.455(3)
b [Å]	12.4969(18)	11.5966(15)	10.537(2)	10.151(2)	10.5405(12)
c [Å]	13.401(2)	20.456(4)	17.204(3)	28.321(6)	17.231(3)
α [°]	70.737(17)	90	90	90	90
β [°]	87.707(18)	121.381(15)	113.55(3)	96.88(3)	113.553(19)
γ [°]	75.065(16)	90	90	90	90
Volume [Å^3], Z	1135.2(3), 2	2230.7(6), 1	2903.9(10), 4	2605.5(9), 4	2906.1(8), 1
F(000)	570	1134	1336	1140	680
Reflections collected	13636	5434	12614	21099	3425
Data/restraints/parameters	5062/0/380	1162/10/296	3463/0/168	5842/0/316	3425/0/162
Goof on F^2	0.911	0.538	0.873	0.883	0.803
Final R indices $[I > 2\sigma(I)]$	R_{int} = 0.049	R_{int} = 0.256	R_{int} = 0.103	R_{int} = 0.048	R_{int} = 0.276
R indices (all data)	R_1 = 0.039, wR_2 = 0.086	R_1 = 0.0772, wR_2 = 0.1646	R_1 = 0.0443, wR_2 = 0.0983	R_1 = 0.036, wR_2 = 0.074	R_1 = 0.192, wR_2 = 0.285
	R_1 = 0.069, wR_2 = 0.094	R_1 = 0.2784, wR_2 = 0.2031	R_1 = 0.0973, wR_2 = 0.1061	R_1 = 0.070, wR_2 = 0.083	R_1 = 0.100, wR_2 = 0.271
Largest difference peak/hole [e Å^{-3}]	0.420/–0.418	0.298/–0.370	0.477/–0.642	0.329/–0.426	1.648/–0.403
CCDC-	701775	701774	701776	701777	701778
M–N	2.045(2), 2.032(2)	2.030(7), 2.261(3)	2.047(3)	1.957(2), 1.958(2)	2.038(10)
M–O	2.153(2), 2.119(2)	2.115(7), 2.069(6)	2.121(3), 2.093(4)	2.173(2), 2.156(2)	2.121(10), 2.126(9)
O–M–O	152.4(1), 146.9(1)	150.4(3), 153.6(3)	152.4(1)	156.8(1), 156.4(1)	153.1(3)
O–M–N	76.1(1), 76.9(1) 75.0(1), 76.9(1)	75.9(3), 77.7(3) 76.7(3), 76.7(3)	76.6(1), 75.9(1)	78.05(8), 78.36(8) 78.44(8), 78.43(8)	76.5(4), 76.6(4)
N–M–N	165.5(1)	172.3(3)	174.5(1)	178.22(8)	174.6(5)
NOOM/NOOM	91.6(1)	91.6(1)	93.2(1)	91.2(1)	94.0(1)

Table 5. Crystal and refinement data and selected bond lengths [Å] and angles [°] for complexes $[(RR'pydimH_2)_2PdCl_2]$ and *cis*- and *trans*-$[(RR'pydimH_2)(dmso)MCl_2]$.

Compound	*trans*-$[(pydimH_2)_2PdCl_2]\cdot 2H_2O$	*cis*-$[(pydimH_2)(dmso)PtCl_2]$	*trans*-$[(pydimH_2)(dmso)PtCl_2]$
Empirical formula	$C_{28}H_{40}Cl_4N_4O_{12}Pd_2$	$C_9H_{15}Cl_2NO_3PtS$	$C_9H_{15}Cl_2NO_3PtS$
Formula mass	979.3 g mol^{-1}	966.5 g mol^{-1}	1933.1 g mol^{-1}
Crystal system	monoclinic	triclinic	monoclinic
Space group	$C2/m$ (No. 12)	$P\bar{1}$ (No. 2)	$P2_1/c$ (No. 14)
a [Å]	7.0674(10)	7.9393(11)	12.5764(16)
b [Å]	15.685(3)	9.1867(13)	8.7029(9)
c [Å]	8.3102(11)	9.6526(14)	13.9796(15)
α [°]	90	92.402(17)	90
β [°]	93.466(16)	95.430(17)	112.527(13)
γ [°]	90°	100.288(17)	90
Volume [Å^3], Z	919.5(3), 1	688.35(17), 1	1413.3(3), 1
F(000)	496	456	912
Reflections collected	4166	7970	13331
Data/restraints/parameters	1098/0/68	3073/0/159	3249/0/159
Goof on F^2	1.117	0.993	0.779
Final R indices $[I > 2\sigma(I)]$	R_1 = 0.0318, wR_2 = 0.0897	R_1 = 0.034, wR_2 = 0.076	R_1 = 0.040, wR_2 = 0.062
R indices (all data)	R_1 = 0.0319, wR_2 = 0.0897	R_1 = 0.043, wR_2 = 0.078	R_1 = 0.097, wR_2 = 0.071
Largest difference peak/hole [e Å^{-3}]	0.430/–0.690	1.462/–1.424	1.336/–1.970
CCDC-	701783	701784	701785
M–N	2.046(3)	2.051(5)	2.065(8)
M–Cl	2.306(1)	2.302(2), 2.295(2)	2.298(2), 2.295(2)
M–S	–	2.200(2)	2.224(3)
Cl–M–Cl	180.00	90.10(7)	175.6(1)
Cl–M–N	90.00(2)	88.0(2), 178.0(2)	87.3(2), 89.0(2)
N–M–N/S	180.00	91.9(2)	177.7(2)
NNClClM/py	99.0(1)	91.8(1)	94.6(1)

tion corrections (X-RED V1.22; Stoe & Cie, 2001) were performed after optimising the crystal shapes by using X-SHAPE V1.06 (Stoe & Cie, 1999).[40] The non-hydrogen atoms were refined with anisotropic displacement parameters without any constraints. The H atoms of the oxo pincer ligands' OH groups were all found during the refinement process, other H atoms were included by using appropriate riding models. For further details see Tables 3, 4 and 5. CCDC-701771, -701772, -701773, -701774, -701775, -701776, -701777, -701778, -701779, -701780, -701781, -701782, -701783, -701784, -701785 contain the supplementary crystallographic data for this paper. These data can be obtained free of charge from The Cambridge Crystallographic Data Centre via www.ccdc.cam.ac.uk/data_request/cif.

Supporting Information (see footnote on the first page of this article): Data from absorption spectroscopy, including selected absorption spectra, the paramagnetically broadened ^{1}H NMR spectrum of [(pydotH_2)NiCl_2], as well as figures for all 15 crystal and molecular structures.

Acknowledgments

Dr. Ingo Pantenburg and Ingrid Müller from the Institute for Inorganic Chemistry are thanked for the X-ray measurements. We are also grateful to Johnson Matthey for a loan of K_2PtCl_4 and K_2PdCl_4.

[1] J. T. Singleton, *Tetrahedron* **2003**, *59*, 1837–1857.
[2] M. Albrecht, G. van Koten, *Angew. Chem.* **2001**, *113*, 3866–3898; *Angew. Chem. Int. Ed.* **2001**, *40*, 3750–3781.
[3] a) J. A. Davies, F. R. Hartley, *Chem. Rev.* **1981**, *81*, 79–90; b) R. G. Pearson, *Inorg. Chem.* **1988**, *27*, 734–740; c) R. G. Pearson, *J. Am. Chem. Soc.* **1963**, *85*, 3533–3539.
[4] J. M. Hawkins, K. B. Sharpless, *Tetrahedron Lett.* **1987**, *28*, 2825–2828.
[5] R. M. Gauvin, J. A. Osborn, J. Kress, *Organometallics* **2000**, *19*, 2944–2946.
[6] P. E. Fanwick, L. M. Kobriger, A. K. McMullen, I. P. Rothwell, *J. Am. Chem. Soc.* **1986**, *108*, 8095–8097.
[7] S. Bellemin-Laponnaz, K. S. Coleman, P. Dierkes, J.-P. Masson, J. A. Osborn, *Eur. J. Inorg. Chem.* **2000**, 1645–1649.
[8] J. M. Hawkins, J. C. Dewan, K. B. Sharpless, *Inorg. Chem.* **1986**, *25*, 1501–1503.
[9] K. V. Zaitsev, M. V. Bermeshev, S. S. Karlov, Y. F. Oprunenko, A. V. Churakov, J. A. K. Howard, G. S. Zaitseva, *Inorg. Chim. Acta* **2007**, *360*, 2507–2512.
[10] R. Fandos, B. Gallego, A. Otero, A. Rodriguez, M. J. Ruiz, P. Terreros, C. Pastor, *Organometallics* **2007**, *26*, 2896–2903.
[11] R. J. Fites, A. T. Yeager, T. L. Sarvela, W. A. Howard, G. Zhu, K. Pang, *Inorg. Chim. Acta* **2006**, *359*, 248–256.
[12] J. M. Berg, R. H. Holm, *Inorg. Chem.* **1983**, *22*, 1768–1771.
[13] a) V. T. Yilmaz, S. Guney, O. Andac, W. T. A. Harrison, *J. Coord. Chem.* **2003**, *56*, 21–32; b) O. Andac, S. Guney, Y. Topcu, V. T. Yilmaz, W. T. A. Harrison, *Acta Crystallogr., Sect. C* **2002**, *58*, m17–m20.
[14] a) S. Winter, W. Seichter, E. Weber, *J. Coord. Chem.* **2004**, *57*, 997–1014; b) S. Winter, W. Seichter, E. Weber, *Z. Anorg. Allg. Chem.* **2004**, *630*, 434–442.
[15] M. Koman, M. Melnik, *Polyhedron* **1997**, *16*, 2721–2726.
[16] M. Melnik, M. Koman, L. Macaskova, T. Glowiak, R. Grobelny, J. Mrozinsky, *J. Coord. Chem.* **1998**, *43*, 159–167.
[17] M. Melnik, C. E. Holloway, *J. Coord. Chem.* **1999**, *49*, 69–73.
[18] M. Koman, M. Melnik, J. Moncol, *Inorg. Chem. Commun.* **2000**, *3*, 262–266.
[19] A. K. Gupta, J. Kim, *Acta Crystallogr., Sect. C* **2003**, *59*, m262-m264.
[20] C. Boskovic, W. Wernsdorfer, K. Folting, J. C. Huffman, D. N. Hendrickson, G. Christou, *Inorg. Chem.* **2002**, *41*, 5107–5118.
[21] a) J. Yoo, E. K. Brechin, A. Yamaguchi, M. Nakano, J. C. Huffman, A. L. Maniero, L.-C. Brunel, K. Awaga, H. Ishimoto, G. Christou, D. N. Hendrickson, *Inorg. Chem.* **2000**, *39*, 3615–3623; b) E. K. Brechin, J. Yoo, M. Nakano, J. C. Huffman, D. N. Hendrickson, G. Christou, *Chem. Commun.* **1999**, 783–784.
[22] S. Onaka, L. Hong, M. Ito, T. Sunahara, H. Imai, K. Inoue, *J. Coord. Chem.* **2005**, *58*, 1523–1530.
[23] T. Kawato, H. Koyama, H. Kanatomi, Y. Muramoto, *Inorg. Chim. Acta* **1991**, *183*, 107–112.
[24] F. D. Rochon, A. L. Beauchamp, C. Bensimon, *Can. J. Chem.* **1996**, *74*, 2121–2130.
[25] a) S. Goto, J. Velder, S. El Sheikh, Y. Sakamoto, M. Mitani, S. Elmas, A. Adler, A. Becker, J.-M. Neudörfl, J. Lex, H.-G. Schmalz, *Synlett* **2008**, *9*, 1361–1365; b) S. El Sheikh, H.-G. Schmalz, *Curr. Opin. Drug Discovery Dev.* **2004**, *7*, 882–894.
[26] E. Gómez, R. Flores, G. Huerta, C. Alvarez-Toledano, R. A. Toscano, V. Santes, N. Nava, P. Sharma, *J. Organomet. Chem.* **2003**, *672*, 115–122.
[27] T. Steiner, *Angew. Chem.* **2002**, *114*, 50–80; *Angew. Chem. Int. Ed.* **2002**, *41*, 48–76.
[28] J. E. Huheey, E. A. Keiter, R. L. Keiter, *Inorganic Chemistry: Principles of Structure and Reactivity*, 4. ed., Harper Collins College Publishers, New York, **1993**.
[29] C. Furlani, *Coord. Chem. Rev.* **1968**, *3*, 141–167.
[30] A. Klein, T. Schurr, A. Knödler, D. Gudat, K.-W. Klinkhammer, V. K. Jain, S. Záliš, W. Kaim, *Organometallics* **2005**, *24*, 4125–4131.
[31] J. R. L. Priqueler, F. D. Rochon, *Inorg. Chim. Acta* **2004**, *357*, 2167–2175.
[32] a) M. R. Plutino, M. L. Scolaro, A. Albinati, R. Romeo, *J. Am. Chem. Soc.* **2004**, *126*, 6470–6484; b) S. Lanza, D. Minniti, P. Moore, J. Sachinidis, R. Romeo, *Inorg. Chem.* **1984**, *23*, 4428–4433.
[33] M. P. Feth, A. Klein, H. Bertagnolli, *Eur. J. Inorg. Chem.* **2003**, 839–852.
[34] *IUPAC Gold Book*, International Union of Pure and Applied Chemistry, **2005–2008**, http://goldbook.iupac.org/index.html.
[35] a) M. Ciamporlini, N. Nardi, *Inorg. Chem.* **1967**, *6*, 445–449; b) M. Ciamporlini, N. Nardi, *Inorg. Chem.* **1966**, *5*, 41–44.
[36] S. E. Manahan, R. T. Iwamoto, *Inorg. Chem.* **1965**, *4*, 1409–1413.
[37] H. Kaczmarek, *J. Photochem. Photobiol. A: Chem.* **1996**, *95*, 61–65.
[38] G. M. Sheldrick, *SHELXS-97: A program for Crystal Structure Resolution*, University of Göttingen, Germany, **1997**.
[39] G. M. Sheldrick, *SHELXL-97: A Program for the Refinement of Crystal Structures*, University of Göttingen, Germany, **1997**.
[40] *STOE X-RED*, Data Reduction Program, Version 1.22/Windows, STOE & Cie, Darmstadt, **2001**; *STOE X-SHAPE*, Crystal Optimisation for Numerical Absorption Correction, Version 1.06/Windows, STOE & Cie, Darmstadt, **1999**.

Received: January 9, 2009
Published Online: April 16, 2009

